

Development of a CSGPS/DR Integrated System for High-precision Trajectory Estimation for the Purpose of Vehicle Navigation

Sang-Hoon Yoo¹, Jeong-Min Lim², Jeong-Hun Oh¹, Ho-Beom Kim², Kwang-Eog Lee³, Tae-Kyung Sung^{1†}

¹Department of Information and Communication Engineering, Chungnam National University, Daejeon 305-764, Korea

²Institute of Technology, Wifive Co. Ltd., Daejeon 305-308, Korea

³National GNSS Research Center, Agency for Defense Development, Daejeon 305-152, Korea

ABSTRACT

In this study, a carrier smoothed global positioning system / dead reckoning (CSGPS/DR) integrated system for high-precision trajectory estimation for the purpose of vehicle navigation was proposed. Existing code-based GPS has a low position accuracy, and carrier-phase differential global positioning system (CPDGPS) has a long waiting time for high-precision positioning and has a problem of high cost due to the establishment of infrastructure. To resolve this, the continuity of a trajectory was guaranteed by integrating CSGPS and DR. The results of the experiment indicated that the trajectory precision of the code-based GPS showed an error performance of more than 30cm, while that of the CSGPS/DR integrated system showed an error performance of less than 10cm. Based on this, it was found that the trajectory precision of the proposed CSGPS/DR integrated system is superior to that of the code-based GPS.

Keywords: GPS, carrier phase, dead-reckoning, integrating, filter

1. INTRODUCTION

In recent years, unmanned autonomous vehicles have drawn global attention. The core of an unmanned autonomous vehicle is advanced driver assistance system (ADAS). In the case of the advanced driver assistance system, a vehicle defines the status of the vehicle by perceiving and interpreting the surrounding environment and position for itself; and by informing the driver about this information, it prevents accidents and helps the driver travel to a destination. Among the element technologies for implementing this system, vehicle navigation technology is an essential element technology, which can accurately figure out the position of a vehicle. If the position obtained

using this is linked with image and road information, it can be applied as a technology for lane keeping and lateral control.

In most vehicle navigation systems, the code measurement of global positioning system (GPS) is utilized. However, the code measurement of GPS has a problem of low trajectory precision. As an alternative to this, a carrier-phase differential global positioning system (CPDGPS) technique using the carrier phase measurement of GPS can be used to obtain a position solution with an accuracy of several centimeters. However, to apply the CPDGPS technique, integer ambiguity included in carrier phase measurement needs to be determined. For this, measurement needs to be collected for several minutes in a stationary state. Also, a reference station with correction information and a communication infrastructure need to be established. Thus, it has disadvantages of distance limitation and a lot of cost.

To resolve this, a carrier smoothed global positioning

Received July 24, 2015 Revised Aug 20, 2015 Accepted Aug 25, 2015

†Corresponding Author

E-mail: tksaint@cnu.ac.kr

Tel: +82-42-821-5660 Fax: +82-42-824-6807

system (CSGPS) technique can be used to obtain a high-precision trajectory with a precision of less than 30 cm and to obtain continuous relative position and attitude. For this, a study on the use of the Hatch filter was performed (Hatch 1982). The Hatch filter combines the carrier phase measurement including a noise of less than 1 cm and integer ambiguity and the code measurement with a noise of 1~2 m based on the complementary Kalman filter, and utilizes the advantages of the two measurements. However, this method cannot guarantee the continuity of a trajectory because the bias included in a position solution could change in case of the change in visible satellites.

On the other hand, dead reckoning (DR) navigation can obtain continuous relative position and attitude for a short time, but has a problem of accumulating position and attitude error element characteristics. Thus, in DR navigation, it is important to determine initial position and attitude, and to correct the error of DR navigation. Therefore, the CSGPS/DR integrated system was designed so that continuity could be guaranteed in case of the change in bias, using the DR navigation solution of a two-dimensional model (Lee 2014). In the present study, this was implemented using a low-cost model, and it was demonstrated that the performance was improved compared to that of code-based GPS.

2. DEVELOPMENT OF A CSGPS/DR INTEGRATED FILTER

2.1 Measurement and Positioning Solution of GPS

GPS was designed and developed with the purpose of obtaining position information at any place in the world. For GPS, measurements are broadly divided into code measurement, carrier phase measurement, and Doppler measurement. Code measurement is repeated at a period of about 300 m and has large noise, while carrier is repeated at a period of about 0.19 m and has smaller noise compared to code measurement. Thus, when carrier phase measurement is used, more accurate position could be obtained compared to when code measurement is used. Doppler measurement is mostly used to estimate velocity, and precise velocity could be obtained because Doppler also uses carrier. The pseudorange obtained through the code tracking loop of a GPS receiver can be expressed as follows (Kaplan & Hegarty 2006).

$$\begin{aligned} \rho_i &= |p_i - p_{GPS}| + c \cdot b_{GPS} + \hat{O}_1 \\ &= \sqrt{(p_{i,x} - p_{GPS,x})^2 + (p_{i,y} - p_{GPS,y})^2 + (p_{i,z} - p_{GPS,z})^2} + c \cdot b_{GPS} + \hat{O}_1 \end{aligned} \quad (1)$$

where $p_i = [p_{i,x} \ p_{i,y} \ p_{i,z}]^T$ is the position of the satellite, $p_{GPS} = [p_{GPS,x} \ p_{GPS,y} \ p_{GPS,z}]^T$ is the position of the GPS receiver, c is the speed of light, b_{GPS} is the clock bias of the receiver, and \hat{O}_1 represents the error due to ionospheric delay, tropospheric delay, orbit information error, and multipath. The error for pseudorange and estimated position can be expressed through linearization using the Taylor series.

$$\delta\rho_i = \rho_i - \hat{\rho}_i = [h_i^T \ 1] \begin{bmatrix} \delta p_{GPS} \\ c \cdot \delta b_{GPS} \end{bmatrix} + \hat{O}_1 \quad (2)$$

where $\hat{\rho}_i = \hat{r}_i + c \cdot \hat{b}_{GPS}$ is the estimated pseudorange, $h_i = [\frac{x_u - x_i}{\hat{r}_i} \ \frac{y_u - y_i}{\hat{r}_i} \ \frac{z_u - z_i}{\hat{r}_i}]^T$ is the line of sight vector, $\hat{r}_i = \sqrt{(p_{i,x} - \hat{p}_{GPS,x})^2 + (p_{i,y} - \hat{p}_{GPS,y})^2 + (p_{i,z} - \hat{p}_{GPS,z})^2}$ is the estimated distance from the satellite, $\delta p_{GPS} = [\delta p_{GPS,x} \ \delta p_{GPS,y} \ \delta p_{GPS,z}]^T$ is the GPS position error, and $\delta x = \hat{x}_u - x_u$, $\delta y = \hat{y}_u - y_u$, $\delta z = \hat{z}_u - z_u$ are the X-, Y-, and Z-axis errors, respectively. When there are more than four visible satellites, unknowns (δp_{GPS} , $c \cdot \delta b_{GPS}$) can be estimated based on the least square method or the Kalman filter, and the position of the receiver can be estimated by renewing the position solution of the receiver. In this study, when the position of a receiver was needed before performing position estimation using carrier measurement, a position estimation technique using code measurement was utilized.

When the carrier phase measurement of GPS is used, the total change in the distance that a vehicle has traveled can be continuously obtained, and precise position measurement is enabled. However, carrier phase measurement includes integer ambiguity, and it is difficult to determine integer ambiguity in real time. When integer ambiguity included in carrier phase measurement is estimated and a carrier smoothed GPS technique that performs navigation using only estimated integer ambiguity and carrier phase measurement is used, a high-precision trajectory where bias is included in the position solution can be obtained. However, for the actual application of a carrier smoothed GPS technique, the change in bias that occurs due to cycle slip or the change in visible satellites needs to be compensated.

If a low-cost receiver using single frequency is used for a carrier smoothed GPS technique, it is difficult to determine integer ambiguity in real time using only carrier phase measurement. However, when the position solution obtained based on pseudorange and the carrier phase measurement are used, integer ambiguity can be estimated using single measurement. Carrier phase measurement is as follows (Kaplan & Hegarty 2006).

$$\Phi_i(k) = \left| \underline{p}_i - \underline{p}_{CSGPS} \right| + \lambda N_i + c \cdot b_{GPS}(k) + \hat{O}_1(k) \quad (3)$$

where \underline{p}_{CSGPS} is the position vector of the receiver estimated based on the carrier smoothed GPS technique, N_i is the integer ambiguity of the i -th satellite, and λ is the wavelength of the carrier, where it is ($c/1.57542$ GHz) in the case of the L1 of GPS.

When GPS measurement differenced between satellites is used, the clock bias of the receiver can be effectively eliminated. The tropospheric and ionospheric errors decrease as the elevation angle increases. Thus, differencing is performed based on a satellite with the highest elevation angle. When the reference satellite is marked as 1, differencing between satellites is performed as follows.

$$\Phi_{i1}(k) = \hat{r}_{i1}(k) + \underline{h}_{i1}^T(k) \delta \underline{p}_{CSGPS}(k) + \lambda N_{i1} + \hat{O}_{i1}(k) \quad (4)$$

where $\Phi_{i1}(k) = \Phi_i(k) - \Phi_1(k)$, $\hat{r}_{i1}(k) = \hat{r}_i(k) - \hat{r}_1(k)$, $\underline{h}_{i1}^T(k) = \underline{h}_i^T(k) - \underline{h}_1^T(k)$, $N_{i1}(k) = N_i(k) - N_1(k)$, and $\hat{O}_{i1}(k) = \hat{O}_i(k) - \hat{O}_1(k)$. If it is assumed that the noise corrected through ephemeris information in a stationary state is negligible (i.e., $\delta \underline{p}_{CSGPS}(k) \approx 0$, $\hat{O}_{i1}(k) \approx 0$), the differenced measurement can be expressed as follows.

$$\Phi_{i1}(k) \approx \hat{r}_{i1}(k) + \lambda N_{i1} \quad (5)$$

The integer ambiguity estimated from the differenced measurement at $k=0$ is as follows.

$$\hat{N}_{i1} = (\Phi_{i1}(0) - \hat{r}_{i1}(0)) / \lambda \quad (6)$$

Assuming that the error terms are negligible, the relationship between estimated integer ambiguity and actual integer ambiguity is as follows, where the error is expressed as a constant.

$$\begin{aligned} \delta N_{i1} &= N_{i1} - \hat{N}_{i1} \\ &= (\hat{O}_{i1}(0) + \underline{h}_{i1}^T(0) \delta \underline{p}_{CSGPS}(0) + c \cdot \delta b_{GPS}(0)) / \lambda \quad (7) \end{aligned}$$

When the estimated integer ambiguity is substituted into the carrier measurement differenced between satellites in order to perform the carrier smoothed GPS technique, it can be expressed as follows.

$$\Phi_{i1}(k) - \hat{r}_{i1}(k) - \lambda \hat{N}_{i1} = \underline{h}_{i1}^T(k) \delta \underline{p}_{CSGPS}(k) + \hat{O}_{i1}(k) + \omega_{N_i} \quad (8)$$

where $\omega_{N_i} = \hat{O}_{i1}(0) + \underline{h}_{i1}^T(0) \delta \underline{p}_{CSGPS}(0) + c \cdot \delta b_{GPS}(0)$ is the integer ambiguity noise of the i -th satellite. This can be expressed using a matrix as follows.

$$\begin{aligned} \Delta \underline{r}_{CS}(k) &= \begin{bmatrix} \Phi_{21}(k) - \hat{r}_{21}(k) - \lambda \hat{N}_{21} \\ \vdots \\ \Phi_{i1}(k) - \hat{r}_{i1}(k) - \lambda \hat{N}_{i1} \end{bmatrix} \\ &= \begin{bmatrix} \underline{h}_{21}^T(k) \\ \vdots \\ \underline{h}_{i1}^T(k) \end{bmatrix} \delta \underline{p}_{CSGPS}(k) + \begin{bmatrix} \hat{O}_{21}(k) \\ \vdots \\ \hat{O}_{i1}(k) \end{bmatrix} + \begin{bmatrix} \omega_{N_2} \\ \vdots \\ \omega_{N_i} \end{bmatrix} \\ &= H_{CS}(k) \delta \underline{p}_{CSGPS}(k) + \hat{O}(k) + \underline{\omega}_N \quad (9) \end{aligned}$$

In addition, the position change, $\delta \underline{p}_{CSGPS}(k)$, is as follows.

$$\delta \underline{p}_{CSGPS}(k) = (H_{CS}^T(k) H_{CS}(k))^{-1} H_{CS}^T(k) (\Delta \underline{r}_{CS}(k) - \hat{O}(k) - \underline{\omega}_N) \quad (10)$$

However, $\hat{O}(k)$, $\underline{\omega}_N$ are not known, and thus the estimated position change, $\delta \hat{\underline{p}}_{CSGPS}(k)$, is as follows.

$$\delta \hat{\underline{p}}_{CSGPS}(k) = (H_{CS}^T(k) H_{CS}(k))^{-1} H_{CS}^T(k) \Delta \underline{r}_{CS}(k) \quad (11)$$

In this regard, the error between the estimated position change and the actual position change is as follows.

$$\delta \hat{\underline{p}}_{CSGPS}(k) - \delta \underline{p}_{CSGPS}(k) = (H_{CS}^T(k) H_{CS}(k))^{-1} H_{CS}^T(k) (\hat{O}(k) + \underline{\omega}_N) \quad (12)$$

If it is assumed that the tropospheric and ionospheric errors hardly change within about 15 minutes where they have a temporal correlation (i.e., $\hat{O}_{i1}(k-1) = \hat{O}_{i1}(k)$), the tropospheric and ionospheric errors depending on time are treated as constants. Then, these are combined with the error from the estimated integer ambiguity, and it appears as if there is a bias in the position solution. However, the troposphere and the ionosphere change with time, and thus the bias included in the position solution changes.

The carrier tracking loop of a GPS receiver provides the difference between the frequencies of the received signal and the signal transmitted from a satellite. This difference is caused by the Doppler effect depending on the movement of the satellite and the receiver, clock drift, and the frequency error of the receiver. The Doppler measurement for the i -th satellite is as follows (Noureldin et al. 2013).

$$f_{d,i} = -\dot{\rho}_i / \lambda \quad (13)$$

where $f_{d,i}$ is the Doppler measurement for the i -th satellite, and $\dot{\rho}_i$ is the pseudorange rate for the i -th satellite and can be expressed as follows (Grewal et al. 2007).

$$\dot{\rho}_i = (\underline{v}_i - \underline{v}_{GPS}) \frac{\underline{p}_i - \underline{p}_{GPS}}{\left| \underline{p}_i - \underline{p}_{GPS} \right|} + c \cdot \dot{b}_{GPS} + \hat{O}_1 \quad (14)$$

where $\underline{v}_i = [v_{i,x} \ v_{i,y} \ v_{i,z}]^T$ is the velocity of the i -th satellite, $\underline{v}_{GPS} = [v_{GPS,x} \ v_{GPS,y} \ v_{GPS,z}]^T$ is the velocity of the GPS receiver, $\dot{\rho}_i$ is the pseudorange rate for the i -th

satellite, and \hat{b}_u is the clock drift of the receiver. The error for the pseudorange rate can be linearized using the Taylor series.

$$\delta\hat{\rho}_i = \hat{\rho}_i - \hat{\rho}_i = [\underline{h}_i^T \quad 1] \begin{bmatrix} \delta\underline{v}_{GPS} \\ c \cdot \delta\hat{b}_{GPS} \end{bmatrix} + \hat{O}_1 \quad (15)$$

where $\hat{\rho}_i = (\underline{v}_i - \underline{\hat{v}}_{GPS})(\underline{p}_i - \underline{\hat{p}}_{GPS}) / (|\underline{p}_i - \underline{\hat{p}}_{GPS}|_i)$ is the estimated pseudorange rate for the i -th satellite, $\delta\underline{v}_{GPS} = [\delta v_{GPS,x} \quad \delta v_{GPS,y} \quad \delta v_{GPS,z}]^T$ is the error of the GPS receiver velocity, and $\delta v_{GPS,x} = \hat{v}_{GPS,x} - v_{GPS,x}$, $\delta v_{GPS,y} = \hat{v}_{GPS,y} - v_{GPS,y}$, $\delta v_{GPS,z} = \hat{v}_{GPS,z} - v_{GPS,z}$ are the position errors of the GPS receiver for the X-, Y-, and Z-axis, respectively. When there are more than four visible satellites, unknowns ($\delta\underline{v}_{GPS}, c \cdot \hat{b}_{GPS}$) can be estimated based on the least square method or the Kalman filter, and the velocity of the receiver can be estimated by renewing the velocity solution of the receiver.

2.2 DR for Vehicles

DR navigation is an independent navigation technique that calculates a relative position compared to a prior position using the attitude and velocity of a vehicle. However, it has a disadvantage of accumulating error with time. Thus, for the actual application of DR navigation, error correction is important. On the other hand, general DR navigation applied to a vehicle is modeled assuming that a vehicle travels on a two-dimensional plane (Titterton & Weston 2004).

In this study, for DR navigation, a gyro sensor and a velocity sensor outputted through on-board diagnostics-II (OBD-II) were used. If there is no error for the initial position of a vehicle and the velocity of the vehicle is accurately known, the position of the vehicle can be expressed by integrating the velocity of the vehicle.

$$\underline{p} = \underline{p}_0 + \int_{t_0}^t \underline{v} dt \quad (16)$$

The velocity of a vehicle in the navigation frame (n-frame: N, E, D) can be expressed using the speed and attitude of the vehicle (Noureldin et al. 2013). Fig. 1 shows the navigation frame of the vehicle in this system.

$$\underline{v} = [v_E \quad v_N \quad v_U]^T = spd [(c(\theta) \cdot s(\psi)) \quad (c(\theta) \cdot c(\psi)) \quad s(\theta)]^T \quad (17)$$

As only X and Y, which represent a position on a plane, were considered, the value of the roll axis was assumed to be 0. v_E, v_N, v_U are the velocities in the east, north, and vertical

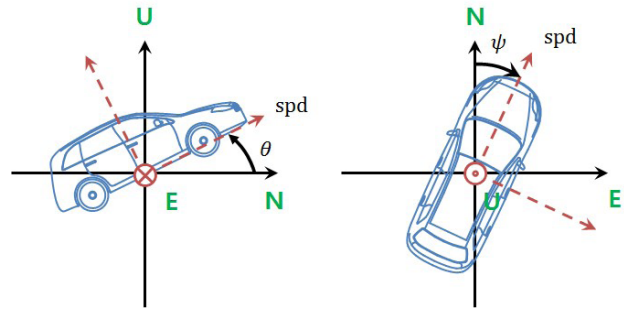


Fig. 1. Definition of the DR coordinate system.

directions, respectively, spd is the speed of the vehicle in the moving direction, and θ, ψ are the climbing angle and attitude angle of the vehicle, respectively. In this study, to obtain the speed of the vehicle in the moving direction and the attitude angle of the vehicle, OBD-II and a gyro sensor were used. The speed of the vehicle in the moving direction using OBD-II can be defined as follows.

$$spd(t_k) = sf_o(t_k) \cdot s_o(t_k) \quad (18)$$

where $spd(t_k)$ is the speed of the vehicle in the moving direction at time t_k , $sf_o(t_k)$ is the conversion factor for the speed of the vehicle in the moving direction outputted from OBD-II, and $s_o(t_k)$ is the speed of the vehicle in the moving direction outputted from OBD-II. The climbing angle and attitude angle of the vehicle can be obtained by integrating the angular velocity, and the angular velocity can be obtained using the output of the gyro sensor.

$$\begin{bmatrix} \phi \\ \theta \\ \psi \end{bmatrix} = sf_{\tilde{\omega}} \begin{bmatrix} 1 & s(\phi)t(\theta) & c(\phi)t(\theta) \\ 0 & c(\phi) & -s(\phi) \\ 0 & \frac{s(\phi)}{c(\theta)} & \frac{c(\phi)}{c(\theta)} \end{bmatrix} \begin{bmatrix} \tilde{\omega}_x - b_{\tilde{\omega}_x} \\ \tilde{\omega}_y - b_{\tilde{\omega}_y} \\ \tilde{\omega}_z - b_{\tilde{\omega}_z} \end{bmatrix} \quad (19)$$

where ϕ, θ, ψ are the angular velocities of each axis, respectively, $sf_{\tilde{\omega}}$ is the conversion factor of the gyro provided by the gyro manufacturer, $\tilde{\omega}_x, \tilde{\omega}_y, \tilde{\omega}_z$ are the angular velocities including bias which are the outputs of the gyro sensor, and $b_{\tilde{\omega}_x}, b_{\tilde{\omega}_y}, b_{\tilde{\omega}_z}$ are the biases of the gyro sensor outputs. If it is assumed that the bias of the each axis of the gyro sensor and the gyro sensor conversion factor are constant during the sampling period for the implementation of a system, the climbing angle and the attitude angle can be obtained as follows.

$$\theta(t_k) \cong \theta(t_{k-1}) + sf_{\tilde{\omega}}(t_{k-1}) \{c(\phi(t_{k-1})) \cdot (\tilde{\omega}_y(t_k) - b_{\tilde{\omega}_y}(t_{k-1}))\} \Delta t - sf_{\tilde{\omega}}(t_{k-1}) \{s(\phi(t_{k-1})) \cdot (\tilde{\omega}_z(t_k) - b_{\tilde{\omega}_z}(t_{k-1}))\} \Delta t \quad (20)$$

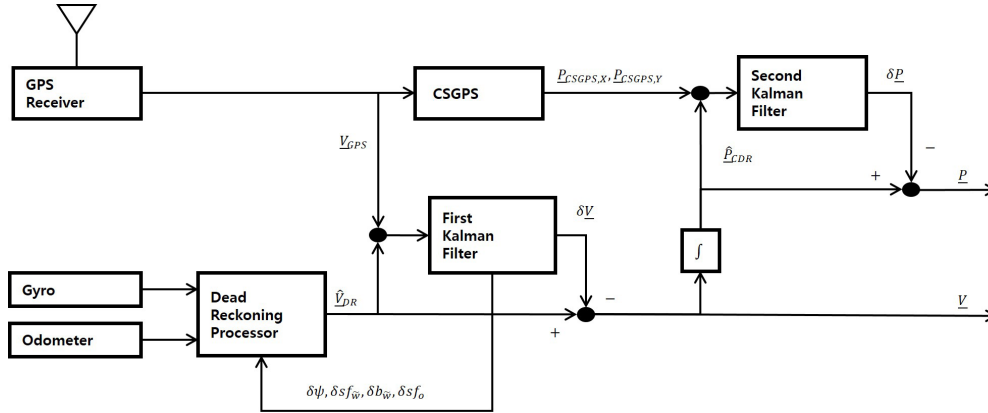


Fig. 2. Structure of the CSGPS/DR integrated Kalman filter.

$$\begin{aligned} \psi(t_k) \cong & \psi(t_{k-1}) + \frac{sf_{\tilde{\omega}}(t_{k-1})}{c(\theta(t_{k-1}))}(t_{k-1}) \{c(\phi(t_{k-1})) \cdot (\tilde{\omega}_y(t_k) - b_{\tilde{\omega}_y}(t_{k-1}))\} \Delta t \\ & + \frac{sf_{\tilde{\omega}}(t_{k-1})}{c(\theta(t_{k-1}))} \{s(\phi(t_{k-1})) \cdot (\tilde{\omega}_z(t_k) - b_{\tilde{\omega}_z}(t_{k-1}))\} \Delta t \end{aligned} \quad (21)$$

where Δt is the sampling period, and the gyro sensor is a digital gyro sensor that outputs the angular velocity at time t_k .

2.3 CSGPS/DR Integrated System for High-precision Trajectory Estimation

The carrier smoothed GPS/DR integrated navigation system combines a carrier smoothed GPS technique that provides precise trajectory and a DR technique that provides a position solution that guarantees continuity for a short time. It can provide more precise trajectory using the advantage of each system even in case of cycle slip or the change in visible satellites, compared to the single use of each system.

To combine each system, they need to be designed so that the models of each system are related to each other. The carrier smoothed GPS/DR system assumes a two-dimensional plane, and thus the roll axis and the pitch axis were not considered. Using the bias error ($\delta b_{\tilde{\omega}_{cz}}$) and conversion factor error ($\delta s f_{\tilde{\omega}}$) of the gyro that corresponds to the yaw axis, the conversion factor error of the odometer ($\delta s f_o$), and the error of the attitude angle ($\delta \psi$), the DR error model was derived as follows.

$$\begin{bmatrix} \delta \psi(k+1) \\ \delta s f_{\tilde{\omega}}(k+1) \\ \delta b_{\tilde{\omega}_{cz}}(k+1) \\ \delta s f_o(k+1) \end{bmatrix} = \begin{bmatrix} 1 & \omega_{cz}(k)\Delta t & -s f_o(k) \cdot \Delta t & 0 \\ 0 & 1 & 0 & 0 \\ 0 & 0 & 1 & 0 \\ 0 & 0 & 0 & 1 \end{bmatrix} \begin{bmatrix} \delta \psi(k) \\ \delta s f_{\tilde{\omega}}(k) \\ \delta b_{\tilde{\omega}_{cz}}(k) \\ \delta s f_o(k) \end{bmatrix} + \begin{bmatrix} w_{\psi}(k) \\ w_{s f_{\tilde{\omega}}}(k) \\ w_{b_{\tilde{\omega}_{cz}}}(k) \\ w_{s f_o}(k) \end{bmatrix} \quad (22)$$

where $\omega_{cz} = \tilde{\omega}_{cz} - b_{\omega_{cz}}$ is the output of the gyro with the correction of the installation error, $\tilde{\omega}_{cz}$ is the angular velocity including bias, $b_{\omega_{cz}}$ is the bias included in $\tilde{\omega}_{cz}$, and $s f_{\tilde{\omega}}$ is the conversion factor of the gyro.

Fig. 2 shows the structure of the loosely coupled carrier

smoothed GPS/DR integrated filter proposed in this study.

Using the first Kalman filter, the error correction and velocity correction for the DR sensor are performed. Then, although the bias included in the position solution of the carrier smoothed GPS changes due to the change in the number of visible satellites, more accurate sensor correction can be performed because the DR sensor is corrected using the GPS carrier velocity information. However, the position solution obtained by integrating the corrected velocity shows error accumulation, and thus the position needs to be corrected using the carrier smoothed GPS position information. Therefore, a position solution is estimated using the velocity information corrected by the first Kalman filter, and the position error is corrected again using the second Kalman filter.

3. EXPERIMENT

The experiment was performed using a CSGPS/DR device from WiFive, Inc., and the positioning performance was examined based on a precise positioning device from Trimble Navigation, Ltd. The performances of the code-based GPS and the CSGPS/DR integrated system were compared. In this regard, the position of the vehicle was obtained using only the measurement with a loss of lock indicator of 0. The precision of a trajectory can be obtained using the standard deviation of a trajectory error, and the trajectory error can be obtained through the following equation.

$$r(k) = \sqrt{dx(k)^2 + dy(k)^2} \quad (23)$$

$$dr(k) = |r(k) - r(0)| \quad (24)$$

In Eq. (23), $dx(k)$ and $dy(k)$ represent the difference between the output position of the product for comparison and the output position of the reference product, and $r(k)$

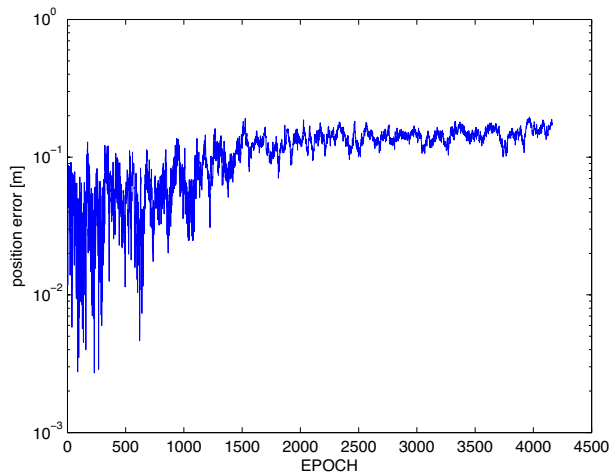


Fig. 3. Comparison of the trajectory errors in a stationary state.

represents the distance between the output position of the product for comparison and the output position of the reference product. In Eq. (24), $dr(k)$ represents the trajectory error, and the trajectory precision can be obtained by calculating the standard deviation of the trajectory error.

3.1 Performance Comparison in a Stationary State

To verify the performance of the CSGPS/DR integrated system in a stationary state, an experiment was performed on the rooftop of a building in Chungnam National University. In the corresponding experiment, data were obtained for about 30 minutes at a spot in a stationary state. As the actual trajectory did not change in a stationary state, comparison was made based on the initial position of the CSGPS/DR integrated system.

Fig. 3 shows the trajectory errors in a stationary state. As shown in this figure, the trajectory precision of the CSGPS/DR integrated system was 4.38 cm, and the error performance was less than 30 cm.

3.2 Performance Comparison in a Straight Section

To compare the performances of the code-based GPS and the CSGPS/DR integrated system in a straight path, an experiment was performed on a test track in the Korea Automotive Technology Institute located in Cheonan. The corresponding test track has a minimum altitude of 42 M and a maximum altitude of 48 M. The experiment consisted of straight driving from the right lower spot to the left upper spot, and the experiment was performed at 30 km/h, 60 km/h, and 80 km/h, respectively. Fig. 4 shows the straight test track and trajectory.

Fig. 5 shows the trajectory errors when driving straight



Fig. 4. Straight test track and trajectory.

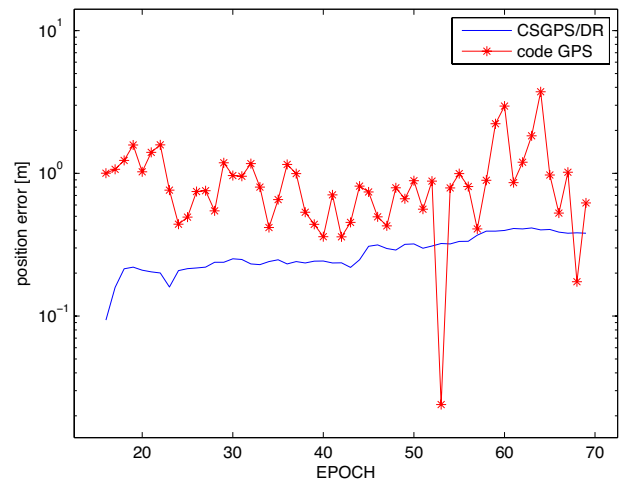


Fig. 5. Comparison of the trajectory errors when driving straight at about 30 km/h.

at about 30km/h. In this case, the trajectory precision of the code-based GPS was 63.47 cm, and that of the CSGPS integrated navigation system was 8.62 cm.

Fig. 6 shows the trajectory errors when driving straight at about 60km/h. In the case, the trajectory precision of the code-based GPS was 51.42 cm, and that of the CSGPS integrated navigation system was 1.78 cm.

Lastly, Fig. 7 shows the trajectory errors when driving straight at about 80km/h. In this case, the trajectory precision of the code-based GPS was 49.30 cm, and that of the CSGPS integrated navigation system was 1.66 cm. In other words, the trajectory precision of the code-based GPS was more than 30 cm regardless of the speed, while that of the CSGPS/DR integrated system was less than 10 cm. Therefore, it was found that the CSGPS/DR integrated system was more precise.

3.3 Performance Comparison in a Path with Curved Sections

To compare the performances of the code-based GPS and the CSGPS/DR integrated system in a curved path,

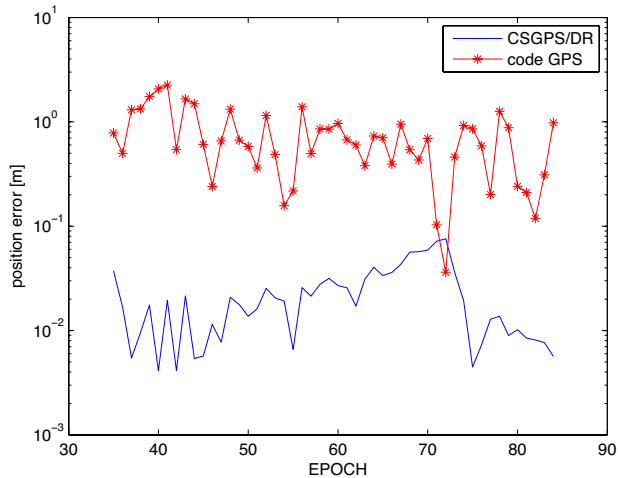


Fig. 6. Comparison of the trajectory errors when driving straight at about 60 km/h.

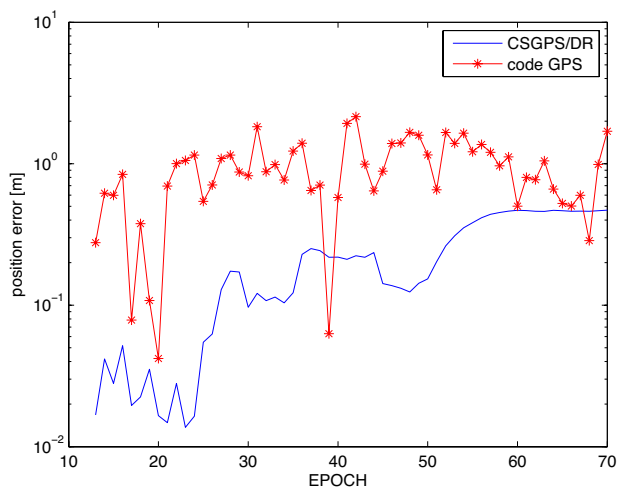


Fig. 7. Comparison of the trajectory errors when driving straight at about 80 km/h.

an experiment was performed on a test track in the Korea Automotive Technology Institute. The corresponding test track has a minimum altitude of 48 M and a maximum altitude of 50 M. The experiment consisted of counterclockwise driving from the left lower spot. Fig. 8 shows the test track and trajectory with curved sections

Fig. 9 shows the trajectory errors when driving on a path with curved sections. In this case, the trajectory precision of the code-based GPS was 109.90 cm, and that of the CSGPS integrated navigation system was 5.34 cm. In other words, the trajectory precision of the code-based GPS was also more than 30 cm, while that of the CSGPS/DR integrated system was less than 10 cm. Therefore, it was found that the CSGPS/DR integrated system was more precise.



Fig. 8. Test track and trajectory with curved sections.

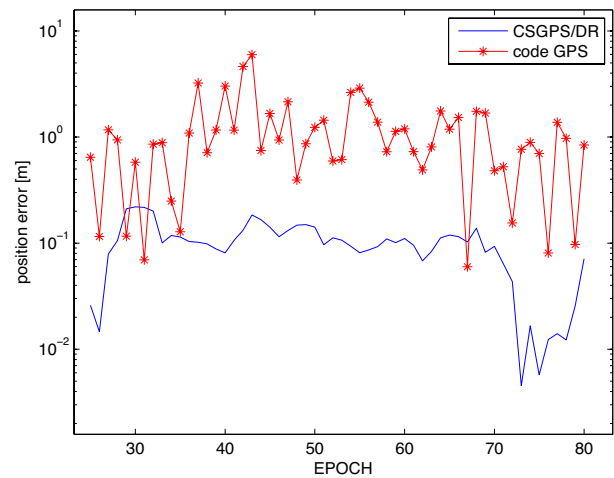


Fig. 9. Comparison of the trajectory errors when driving on a path with curved sections.

4. CONCLUSIONS

In this study, a navigation system that combined a carrier smoothed GPS technique using a low-cost GPS receiver and DR using a low-cost inertial sensor was proposed. Problems for the actual application of the carrier smoothed GPS and the DR were presented, respectively; and to resolve these, a CSGPS/DR integrated navigation system was proposed. In particular, in the case of the carrier smoothed GPS, the bias included in a position solution could change due to the change in visible satellites or cycle slip. Thus, using a DR navigation solution, it was designed so that continuity could be guaranteed in case of the change in the bias. The results of the experiment showed that the trajectory precision of the code-based GPS was more than 30 cm and that of the CSGPS/DR integrated system was less than 10 cm. Based on this, it was found that the CSGPS/DR integrated system has superior performance. Therefore, the proposed CSGPS/DR integrated system for high-precision trajectory estimation

could be applied as the ADAS of autonomous vehicles or as a lane keeping system (e.g., lateral control) if the initial bias error is eliminated using an additional method such as image information. In the future, studies on a three-dimensional model need to be performed.

ACKNOWLEDGMENTS

This work has been supported by the National GNSS Research Center program of Defense Acquisition Program Administration and Agency for Defense Development.

REFERENCES

Grewal, M. S., Weill, L. R., & Andrews, A. P. 2007, *Global Positioning Systems, Inertial Navigation, and Integration*, 2nd ed. (New Jersey: WILEY), pp.92-93

Hatch, R. 1982, The synergism of GPS code and carrier measurements, *Proceedings of the Third International Geodetic Symposium on Satellite Doppler Positioning*, vol. 2, pp.1213-1232. <http://www.gbv.de/dms/tib-ub-hannover/488180333.pdf>

Kaplan, E. D. & Hegarty, C. J. 2006, *Understand GPS principles and applications*, 2nd ed. (Norwood: Artech house), pp.51-58. http://d1.amobbs.com/bbs_upload782111/files_33/ourdev_584835O21W59.pdf

Lee, K. J. 2014, *Implementation and Performance analysis of Carrier-smoothed GPS/DR Integration System*, M.S Dissertation, Chungnam National University

Noureldin, A., Karamat, T. B., & Georgy, J. 2013, *Fundamentals of Inertial Navigation, Satellite-based Positioning and their Integration* (Berlin: Springer), p.105. <http://dx.doi.org/10.1007/978-3-642-30466-8>

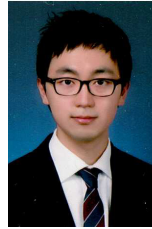
Titterton, D. H. & Weston, J. L. 2004, *Strapdown inertial navigation technology*, 2nd ed. (London: The Institution of Engineering and Technology), pp.19-23



Sang-Hoon Yoo received M.S degree in Information and Communication Engineering from Chungnam National University in 2015. He is a Ph.D student in Information and Communication Engineering from Chungnam National University. His research interests are GPS/GNSS, indoor positioning and Map-Matching.



Jeong-Min Lim received M.S degree in Information and Communication Engineering from Chungnam National University in 2013. He is a Ph.D student in Information and Communication Engineering from Chungnam National University. His research interests are realtime kinematic (RTK) and precise point positioning (PPP).



Jeong-Hun Oh received M.S degree in Information and Communication Engineering from Chungnam National University in 2015. He is a Ph.D student in Information and Communication Engineering from Chungnam National University. His research interests are Multilateration and UWB WPAN positioning, and location signal processing.



Ho-Beom Kim received B.S degree in electrical Engineering from Chungbuk National University in 2014. He is an Engineer of WiFive. His research interests is GPS/GNSS.



Kwang-Eog Lee received B.S., and M.S. degree in electronical engineering from Kyungpook National University, Korea, in 1988 and 1993. He is currently working in Agency for Defense Development (ADD). His research interests are cognitive radio, dynamic spectrum access in tactical satellite/ground communication



Tae-Kyung Sung received B.S., M.S., and Ph.D. degree in control and instrumentation engineering from Seoul National University. After working at the Institute for Advanced Engineering, and Samsung Electronics Co., he joined the Chungnam National University, Daejeon, Korea, where he is currently a Professor of the Division of Electrical and Computer Engineering. He participated in several research projects in the area of positioning and navigation systems. His research interests are GPS/GNSS, Geo-location, UWB WPAN positioning, and location signal processing